APPLIED ORGANOMETALLIC CHEMISTRY
Appl. Organometal. Chem. 2007; **21**: 763–771

(www.interscience.wiley.com) DOI:10.1002/aoc.1262

Synthesis, characterization and soft transformation of some bis(cyclopentadienyl) Ti(IV) and Zr(IV) complexes of Schiff's base ligands to nano-sized titania or zirconia materials

Namita Sharma[1], Vinita Sharma[1], Rakesh Bohra[1]* and V. S. Raju[2]

[1]Department of Chemistry, University of Rajasthan, Jaipur 302004, India
[2]National Center for Compositional Characterization of Materials, Bhabha Atomic Research Center, Hyderabad-500062, India

Received 26 February 2007; Revised 22 March 2007; Accepted 22 March 2007

Some bis(cyclopentadienyl) complexes of Ti(IV)and Zr(IV) have been synthesized by the metathetical reactions of Cp_2MCl_2 with the sodium salt of monofunctional bidentate Schiff's base ligands in 1:1 and 1:2 stoichiometry in anhydrous THF. All the derivatives of the types $Cp_2MCl_{2-n}\{O(C_6H_4)CH{=}NC_6H_5\}_n$ and $Cp_2MCl_{2-n}\{OC(CH_3){=}CHC(R){=}NC_6H_5\}_n$ (where R = CH_3 or C_6H_5 and $n = 1$ or 2) have been characterized by elemental analyses, molecular weight measurements, FT-IR and -NMR [^1H and $^{13}C\{^1H\}$] studies. The FAB mass spectra of a few representative complexes and the molecular weight measurements in freezing benzene indicate their monomeric nature in solution. Spectral studies appear to indicate mono- and bi-dentate mode of attachment of the ligand in solution and in the solid state, respectively. Thermogravimetric analyses (TGA) of $Cp_2TiCl\{O(C_6H_4)CH{=}NPh\}$ (1) and $Cp_2ZrCl\{O(C_6H_4)CH{=}NPh\}$ (7) indicate their low thermal stability. Transformations of some of these complexes to pure titania (TiO_2)/zirconia (ZrO_2) have been observed at relatively low sintering temperatures. Powder X-ray diffraction (XRD) and scanning electron micrograph (SEM) studies suggest the nanocrystalline nature of these materials. Copyright © 2007 John Wiley & Sons, Ltd.

KEYWORDS: nanocrystalline; XRD; SEM; TGA

INTRODUCTION

Metallocene complexes of titanium and zirconium have been recognized as the single-site catalytically active species in metallocene based olefin polymerization catalysis.[1–13] These complexes also exhibit significant biological activities such as antitumor, antiviral, antiflammatory, insecticidal etc.[14–21]

The coordination chemistry of metallocene complexes derived from various multidentate organic ligands has shown interesting structural features.[22–30] Out of these, Schiff's base ligand system attracts considerable research attention due to its remarkable structural diversity associated with its large variety of catalytic and potential biological applications.[31] Our previous studies on Schiff's base derivatives of some transition and non-transition metals have shown a variety of interesting structural patterns.[32–36]

Since the chemically modified metal alkoxides of Ti(IV)[37] and Zr(IV)[38] appear to be better precursors for material synthesis, hydrolytic studies of some of the above complexes using sol–gel technique have also been carried out for the preparation of pure nanosized metal-oxides.

RESULTS AND DISCUSSION

When reactions of Cp_2TiCl_2 with the sodium salt of a Schiff's base (prepared *in situ* by the reaction of NaOMe with Schiff's base in anhydrous MeOH) was carried out in 1 : 1 or 1 : 2 molar

---

*Correspondence to: Rakesh Bohra, Department of Chemistry, University of Rajasthan, Jaipur 302004, India.
E-mail: rkbohra@satyam.net.in
Contract/grant sponsor: UGC.
Contract/grant sponsor: CSIR.
Contract/grant sponsor: DST-New Delhi.

ratio in anhydrous THF, elimination of the Cp groups was observed. This observation is consistent with the literature reports that the elimination of Cp group takes place easily in the presence of protonic nucleophiles or electrofiles.[39,40] However, metathetical reactions of Cp_2TiCl_2 or Cp_2ZrCl_2 with the sodium salts of Schiff's bases in 1 : 1 and 1 : 2 molar ratios in anhydrous THF yielded complexes of the following type:

$$Cp_2MCl_2 + n\,NaL \xrightarrow{THF} Cp_2MCl_{2-n}L_n + n\,NaCl \downarrow$$

where M = Ti or Zr; $L = O(C_6H_4)CH{=}NC_6H_5$ or $OC(CH_3){=}CHC(R){=}NC_6H_5$; $R = CH_3$, or C_6H_5 and $n = 1$ or 2.

All the above reactions are quantitative and the products could be separated easily without the addition of activated neutral alumina.[22] The products are reddish brown solids with sharp melting points (Table 1). Solubility of zirconocene complexes is poor as compared with titanocene complexes in common organic solvents. Molecular weight measurements of titanocene derivatives indicate the monomeric nature of all these complexes in freezing benzene. FAB mass spectra of a few representative titanocene and zirconocene complexes based on Cl-37 isotope (Table 2) also suggest the monomeric nature of these complexes. The appearance of some peaks at higher *m/e* values in comparison to that of the molecular ion peak may be due to reassociation of the fragmented ions.

Spectral studies

IR spectra

Important IR absorption bands of all these complexes are summarized in Table 3. The assignments were made by comparing the IR spectra of the metallocene complexes with those of the free ligands and related derivatives.[33,35] The absence of hydroxy group absorptions of the ligands in the region around 3200 cm^{-1} in all these derivatives indicates deprotonation of the OH group and concomitant bond formation of the ligand moieties with the metal atom. The formation of an M–O bond is further supported by the appearance of a new strong intensity band in the regions, 520–550 cm^{-1} in titanocene complexes and 500–524 cm^{-1} in zirconocene complexes assigned to υ(Ti–O) and υ(Zr–O), respectively.[20] The shifting of υ(C=N) stretching frequencies towards lower wave numbers (30–70 cm^{-1}), as compared with that of the free ligand, indicates coordination of nitrogen atom of the ligand to the central metal atom in the solid state.[32,33] This was further confirmed by the appearance of a new absorption in the region 472–496 cm^{-1} in titanium complexes and 462–479 cm^{-1} in zirconium complexes assigned to υ(M–N) mode.[17] Absorptions around 2900, 1450, 1025 and 830 cm^{-1} are assigned to υ(C–H) (stretching), υ(C–C), υ(C–H) (out of plane bending) and υ(C–H) (in plane bending) modes, respectively, for the Cp ring, indicating the π bonding mode of attachment of the Cp groups to the metal atom in all these complexes.[20]

NMR spectra

The ^1H and $^{13}C\{^1H\}$ NMR spectral data of all these derivatives are summarized in Table 4. A comparison of the ^1H NMR spectra of the complexes with that of the free Schiff's bases[35] shows the absence of —OH signals (in the region δ 12.48–13.31 ppm), indicating deprotonation of ligand moieties and formation of an M–O bond. In all the complexes a single sharp peak in the region δ 6.59–6.61 ppm for titanium(IV)[23,26] and δ 6.31–6.34 ppm for zirconium(IV) complexes[7,8] due to the Cp group was observed in the ^1H NMR spectra except for Cp_2Ti(Schiff's base)$_2$, where a broad peak (δ 6.61–6.78 ppm) was observed. In $^{13}C\{^1H\}$ NMR spectra of all these derivatives only a single resonance at δ 119.0–120.3 for titanium(IV) and at δ 112.7–115.0 for zirconium(IV) derivatives due to the Cp groups was observed.

The absence of any significant shift in the azomethine proton or carbon resonances suggests non-participation of the CH=N nitrogen atom in coordination with the central titanium or zirconium atoms in solution. Similarly ^1H NMR spectra of these derivatives exhibit characteristic peaks and peak multiplicities of the other ligand protons at their expected positions. Carbon resonances also appeared at their expected position in the $^{13}C\{^1H\}$ NMR spectra.[32–36] These observations suggest tetrahedral coordination geometry around the titanium/zirconium atom in all these complexes and Schiff's base is behaving as a monodentate ligand, probably due to steric crowding at the metal center in the solution state.

Unsuccessful attempts have been made to crystallize these products. However, no suitable crystals could be obtained. Although it is difficult to comment on the actual solid-state structure of complexes without single crystal X-ray diffraction study of at least one of the complexes, yet on the basis of IR and NMR studies, bidentate chelating mode of attachment of the ligand in the solid state and monodentate mode of attachment in the solution state may be proposed. In solution the coordination geometry around the central metal atom may be described as a distorted tetrahedron, consisting of ML,Cl/ML,O and the centroids of two Cp rings as the core of tetrahedron. The tentative structures in Fig. 1 may be proposed for all these complexes in the solution state.

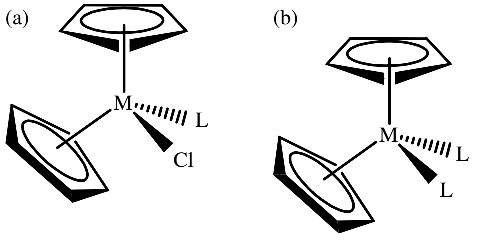

Figure 1. Proposed structures for (a) Cp_2MClL and (b) Cp_2ML_2, where M = Ti or Zr; $L = O(C_6H_4)CH{=}NC_6H_5$ or $OC(CH_3){=}CHC(R){=}NC_6H_5$; $R = CH_3$, or C_6H_5 and $n = 1$ or 2.

Table 1. Synthetic and analytical data of Cp_2MCl_{2-n}\{Schiff's base\}$_n$(M = Ti and Zr; n = 1 or 2)

Reactants (g)					Elemental analyses (%) found (calcd)						
Cp_2MCl_2	NaL	Molar ratio	Complex	Color, state and yield (g)	C	H	N	Cl	Metal	MW found (calcd)	m.p. (°C)
2.33	2.05	1 : 1	$Cp_2TiCl\{O(C_6H_4)CH{=}NPh\}$ (**1**)	Reddish brown solid (3.59)	67.4 (67.4)	4.9 (4.9)	3.4 (3.4)	8.6 (8.6)	11.7 (11.8)	447.7 (409.1)	116
2.20	3.90	1 : 2	$Cp_2Ti\{O(C_6H_4)CH{=}NPh\}_2$ (**2**)	Reddish brown solid (4.75)	75.5 (75.7)	5.4 (5.3)	4.9 (4.9)	—	8.4 (8.4)	563.9 (570.5)	88
2.64	2.09	1 : 1	$Cp_2TiCl\{OC(CH_3){=}CH.C(CH_3){=}NPh\}$ (**3**)	Reddish brown solid (4.01)	69.1 (69.4)	5.7 (5.7)	3.6 (3.6)	9.1 (9.1)	12.3 (12.4)	365.2 (387.6)	120
2.20	3.48	1 : 2	$Cp_2Ti\{OC(CH_3){=}CH.C(CH_3){=}NPh\}_2$ (**4**)	Reddish brown Sticky solid (4.64)	72.8 (73.0)	6.5 (6.5)	2.6 (2.6)	—	9.1 (9.1)	506.3 (526.5)	—
2.07	2.16	1 : 1	$Cp_2TiCl\{OC(CH_3){=}CH.C(C_6H_5){=}NPh\}$ (**5**)	Reddish brown solid (3.72)	69.3 (69.4)	5.3 (5.4)	3.1 (3.1)	7.8 (7.8)	10.6 (10.6)	452.9 (449.8)	79
3.14	1.50	1 : 2	$Cp_2Ti\{OC(CH_3){=}CH.C(C_6H_5){=}NPh\}_2$ (**6**)	Reddish brown solid (3.92)	77.4 (77.5)	5.7 (5.8)	4.3 (4.3)	—	7.4 (7.4)	688.7 (650.7)	76
2.95	2.21	1 : 1	$Cp_2ZrCl\{O(C_6H_4)CH{=}NPh\}$ (**7**)	Yellowish brown solid (4.50)	60.9 (61.0)	4.4 (4.4)	3.0 (3.1)	7.7 (7.8)	20.1 (20.2)	—	85
1.33	1.99	1 : 2	$Cp_2Zr\{O(C_6H_4)CH{=}NPh\}_2$ (**8**)	Yellowish brown solid (2.67)	70.3 (70.4)	4.9 (4.9)	4.5 (4.5)	—	14.8 (14.9)	—	135
2.31	1.56	1 : 1	$Cp_2ZrCl\{OC(CH_3){=}CH.C(CH_3){=}NPh\}$ (**9**)	Brown solid (3.39)	58.5 (58.5)	5.1 (5.1)	3.1 (3.2)	8.2 (8.2)	21.1 (21.2)	—	102
1.81	2.45	1 : 2	$Cp_2Zr\{OC(CH_3){=}CH.C(CH_3){=}NPh\}_2$ (**10**)	Brown sticky solid (3.52)	67.3 (67.4)	5.9 (6.0)	4.8 (4.9)	—	16.1 (16.0)	—	—
1.76	1.56	1 : 1	$Cp_2ZrCl\{OC(CH_3){=}CH.C(C_6H_5){=}NPh\}$ (**11**)	Brown solid (2.86)	63.1 (63.3)	4.8 (4.9)	2.8 (2.8)	7.1 (7.2)	18.5 (18.5)	—	105
1.24	2.21	1 : 2	$Cp_2Zr\{OC(CH_3){=}CH.C(C_6H_5){=}NPh\}_2$ (**12**)	Yellowish brown solid (2.82)	72.6 (72.7)	5.5 (5.5)	3.9 (4.0)	—	13.2 (13.1)	—	100

Table 2. FAB mass spectra of $Cp_2TiCl\{O(C_6H_4)CH{=}NPh\}$ (**1**), $Cp_2Ti\{O(C_6H_4)CH{=}NPh\}_2$ (**2**), $Cp_2ZrCl\{OC(CH_3){=}CH.C(C_6H_5){=}NPh\}$ (**11**) and $Cp_2Zr\{OC(CH_3){=}CH.C(C_6H_5){=}NPh\}_2$ (**12**)

Complex	Fragmented ions	*m*/*e* value
1	$[Cp_2TiCl\{O(C_6H_4)CH{=}NPh\}]^{+1}$	410
	$[Cp_2TiCl\{C_4CH{=}NPh\}]^+$	365
	$[Cp_2TiCl\{C_4CH{=}NC_3H_2\}]^+$	326
	$[Cp_2TiCl\{CH{=}NH_2\}]^+$	242
	$[Cp_2TiCl]^+$	213
2	$[Cp_2Ti\{O(C_6H_4)CH{=}NPh\}_2]^+$	570
	$[Cp_2Ti\{O(C_6H_4)CH{=}NPh\}\{O(C_6H_4)CH{=}NC_2H_2\}]^+$	519
	$[Cp_2Ti\{O(C_6H_4)CH{=}NPh\}\{O(C_6H_4)CH{=}N\}]^+$	493
	$[Cp_2Ti\{O(C_6H_4)CH{=}NPh\}\{O(C_4H_2)\}]^+$	440
	$[Cp_2Ti\{O(C_6H_4)CH{=}NPh\}\{OH\}]^+$	391
	$[CpTi\{O(C_6H_4)CH(C_2H_6)\}]^+$	262
	$[CpTi\{O(C_5H_4)\}]^+$	207
11	$[Cp_2ZrCl\{OC(CH_3){=}CH.C(C_6H_5){=}NPh\}]^+$	491
	$[Cp_2Zr\{OC(CH_3){=}CH.CH_2{=}NPh\}]^+$	381
	$[CpZr\{OCH_2\}]^+$	281
12	$[Cp_2Zr\{OC(CH_3){=}CH.C(C_6H_5){=}NPh\}_2]^+$	692
	$[Cp_2Zr\{OC(CH_3){=}CH.C(C_6H_5){=}NPh\}\{H_3O\}]^+$	475
	$[Cp_2Zr\{OC(CH)C(C_6H_5){=}NPh\}\{H_3O\}]^+$	460
	$[Cp_2Zr\{OC_3(C_6H_5){=}NPh\}\{O\}]^+$	391
	$[Cp_2Zr\{OC_3(C_6H_5){=}NC_6H_3\}]^+$	373

Table 3. IR spectral data of $Cp_2MCl_{2-n}\{\text{Schiff's base}\}_n$ (M = Ti and Zr; $n = 1$ or 2)

Complex no.	ν (C=N)	ν (M–N)	ν (M–O)	C_5H_5
1	1600	472	550	2924, 1445, 1020, 820
2	1620	480	541	2916, 1468, 1029, 858
3	1546	476	540	2900, 1440, 1020, 820
4	1536	478	520	2880, 1440, 1018, 818
5	1552	496	536	2900, 1433, 1052, 828
6	1546	491	545	2900, 1444, 1026, 856
7	1640	468	524	2934, 1440, 1020, 820
8	1648	478	520	2932, 1444, 1036, 822
9	1544	464	522	2930, 1440, 1022, 816
10	1520	462	500	2934, 1438, 1032, 810
11	1550	479	520	2936, 1436, 1018, 824
12	1544	476	522	2934, 1438, 1034, 810

All the vibrations are of strong intensity.

Thermal studies

Thermogravimetric analyses of $Cp_2TiCl\{O(C_6H_4)CH{=}NPh\}$ (**1**) and $Cp_2ZrCl\{O(C_6H_4)CH{=}NPh\}$ (**7**) reveal the low thermal stability of these complexes (Fig. 2). The curves also indicate large thermal events with the increase in the temperature resulting in the pyrolysis of organic moieties attached to the metal atoms. Although it is difficult to comment on the formation of the final species at 900 °C, yet on the basis of percentage mass loss on the TG curves of **1** and **7**, TiO_2 and ZrO_2 do not appear to be the final stable species. The preservation of cyclopentadienyl ligand through thermal treatment to 900 °C is quite improbable, yet formation of CpMO(Cl) as the final species cannot completely be ruled out in view of the fact that Roskey *et al.*[41] reported preparation, crystal and molecular structure of a similar product $[Cp^*TiF(\mu\text{-}O)]_4$ without any comment on its thermal stability.

Hydrolytic studies

Hydrolysis of three representative derivatives $Cp_2TiCl\{O(C_6H_4)CH{=}NPh\}$ (**1**), $Cp_2Ti\{O(C_6H_4)CH{=}NPh\}_2$ (**2**) and $Cp_2ZrCl\{O(C_6H_4)CH{=}NPh\}$ (**7**) was carried out using sol–gel technique. The compounds **2** and **7** were hydrolyzed in the presence of ammonia and **1** in the absence of ammonia. The targeted materials TiO_2 (obtained from **2**) and ZrO_2 (obtained from **7**) were sintered at 600 °C. The TiO_2 (obtained from **1**) was sintered at 900 °C. XRD patterns of TiO_2 and ZrO_2 powders have shown the crystalline nature of the products (Fig. 3). Calculations of the average particle size, using the Debye Scherrer equation[42] from the three major peaks of XRD spectra, indicate the formation of nano-sized particles (10.73 nm for TiO_2 obtained from **2,** 51.67 nm for TiO_2 obtained from **1** and 6.93 nm for ZrO_2 obtained from **7**). A perusal of the SEM images [Fig. 4 (a–c)] of these oxides also shows the formation of microscale agglomerates of the nanocrystalline materials of titania and zirconia. It

DOI: 10.1002/aoc

Table 4. ^{1}H and ^{13}C{^{1}H} NMR spectral data of Cp_2MCl_{2-n}\{Schiff's base\}$_n$ (M = Ti and Zr; *n* = 1 or 2)

Complex	^{1}H NMR (δ ppm)	^{13}C{^{1}H} NMR (δ ppm)
$Cp_2TiCl\{O(C_6H_4)CH{=}NPh\}$ (**1**)	6.61 (s, 10H, Cp); 6.93–7.46 (m, 9H, all phenyl); 8.64 (s, 1H, CH=N)	115.1–134.4 (all aromatic carbons including the signal for Cp at 119.9); 160.8 (CH=N)
$Cp_2Ti\{O(C_6H_4)CH{=}NPh\}_2$ (**2**)	6.70 (b,10H, Cp); 6.91–7.46 (m, 18H, all phenyl); 8.64 (s, 2H, CH=N)	116.0–135.7 (all aromatic carbons including the signal at 119.0 for Cp); 160.8 (CH=N)
$Cp_2TiCl\{OC(CH_3){=}CH.C(CH_3){=}NPh\}$ (**3**)	2.00 (s, 3H, CCH_3); 2.14 (s, 3H, OCCH_3); 5.19 (s, 1H, =CH); 6.59 (s, 10H, Cp); 7.10–7.37 (m, 5H, phenyl)	19.6 (CCH_3); 28.9 (OCCH_3); 97.3 (=CH); 119.9 (Cp); 124.4–138.4 (all aromatic carbons); 159.8 (C=N); 195.8 (CO)
$Cp_2Ti\{OC(CH_3){=}CH.C(CH_3){=}NPh\}_2$ (**4**)	1.99 (s, 6H, CCH_3); 2.16 (s, 6H, OCCH_3); 5.19 (s, 2H, =CH); 6.78 (br, 10H, Cp); 7.09–7.52 (m, 10H, phenyl)	19.7 (CCH_3); 29.0 (OCCH_3); 97.5 (=CH); 119.8 (Cp); 123.8–138.6 (all aromatic carbons); 160.4 (CH=N); 196.1 (CO)
$Cp_2TiCl\{OC(CH_3){=}CH.C(C_6H_5){=}NPh\}$ (**5**)	2.16 (s, 3H, CH_3); 5.90 (s, 1H, =CH); 6.59 (s, 10H, Cp); 7.17–7.43 (m, 5H, N-phenyl); 7.87–7.94 (m, 5H, phenyl)	20.4 (CH_3); 94.3 (=CH); 120.3 (Cp); 123.7–139.0 (all aromatic carbons); 161.9 (C=N); 194.0 (CO)
$Cp_2Ti\{OC(CH_3){=}CH.C(C_6H_5){=}NPh\}_2$ (**6**)	2.13 (s, 6H, CH_3); 5.90 (s, 2H, =CH); 6.76 (br, 10H, Cp); 7.17–7.47 (m, 10H, N-phenyl); 7.87–7.94 (m, 10H, phenyl)	20.1 (CH_3); 93.9 (=CH); 120.0 (Cp); 124.4–139.6 (all aromatic carbons); 162.0 (C=N); 188.2 (CO)
$Cp_2ZrCl\{O(C_6H_4)CH{=}NPh\}$ (**7**)	6.34 (s, 10H, Cp); 6.95–7.29 (m, 9H, all phenyl); 8.00 (s, 1H, CH=N)	114.5 (Cp); 115.7–136.3 (all aromatic carbons); 160.7 (CH=N)
$Cp_2Zr\{O(C_6H_4)CH{=}NPh\}_2$ (**8**)	6.31 (s, 10H, Cp); 6.92–7.45 (m, 18H, all phenyl); 8.62 (s, 2H, CH=N)	115.0 (Cp); 117.2–135.1 (all aromatic carbons); 161.1 (CH=N)
$Cp_2ZrCl\{OC(CH_3){=}CH.C(CH_3){=}NPh\}$ (**9**)	1.91 (s, 3H, CCH_3); 2.17 (s, 3H, OCCH_3); 5.19 (s, 1H, =CH); 6.33 (s, 10H,Cp); 6.79–7.36 (m, 5H, phenyl)	19.0 (CCH_3); 28.4 (OCCH_3); 96.9 (=CH); 113.3 (Cp); 123.6–132.3 (all aromatic carbons); 159.4 (C=N); 192.0 (CO)
$Cp_2Zr\{OC(CH_3){=}CH.C(CH_3){=}NPh\}_2$ (**10**)	1.99 (s, 6H, CCH_3); 2.18 (s, 6H, OCCH_3); 5.19 (s, 2H, =CH); 6.34 (s, 10H, Cp); 7.10–7.36 (m, 10H, phenyl)	19.8 (CCH_3); 29.1 (OCCH_3); 97.5 (=CH); 112.7 (Cp); 124.6–138.6 (all aromatic carbons); 160.2 (C=N); 196.1 (CO)
$Cp_2ZrCl\{OC(CH_3){=}CH.C(C_6H_5){=}NPh\}$ (**11**)	2.15 (s, 3H, CH_3); 5.90 (s, 1H, =CH); 6.31 (s, 10H, Cp); 7.17–7.43 (m, 5H, N-phenyl); 7.87–7.94 (m, 5H, phenyl)	20.3 (CH_3); 94.1 (=CH); 113.9 (Cp); 124.5–139.8 (all aromatic carbons); 162.1 (C=N); 188.4 (CO)
$Cp_2Zr\{OC(CH_3){=}CH.C(C_6H_5){=}NPh\}_2$ (**12**)	2.15 (s, 6H, CH_3); 5.90 (s, 5H, =CH); 6.33 (s, 10H, Cp); 7.17–7.47 (m, 10H, N-phenyl); 7.87–7.94 (m, 10H, phenyl)	20.4 (CH_3); 94.2 (=CH); 114.0 (Cp); 124.7–139.5 (all aromatic carbons); 162.2 (C=N); 188.6 (CO)

is worthwhile mentioning here that smaller particle size was obtained from the routes when ammonia was added during hydrolysis. The TiO_2 obtained from **2** and sintered at 600 °C shows predominant formation of anatase phase while the TiO_2 obtained from **1** and sintered at 900 °C exhibits the presence of both anatase and rutile phases. The ZrO_2 obtained from **7** and sintered at 600 °C exhibits tetragonal phase. Both the secondary electron (SE) and back-scattered electron (BSE) images show the formation of TiO_2 crystals formed completely in the case of sample **1** (obtained from **1** and sintered at 900 °C), while in the case of sample **2** (obtained from **2** sintered at 600 °C), these exhibit the formation of some crystalline features at smaller grains with the bulk of the material seen without crystallinity (Fig. 4).

This is supported by XRD results where XRD spectrum of the sample **1** shows narrow lines exhibiting fully formed crystalline features with the grain size at 51 nm, while the sample **2** (600 °C) shows broad peaks and relatively high noise background, indicating lack of complete crystallinity. The BSE images of sample **1** (900 °C) show clear faces indicating the

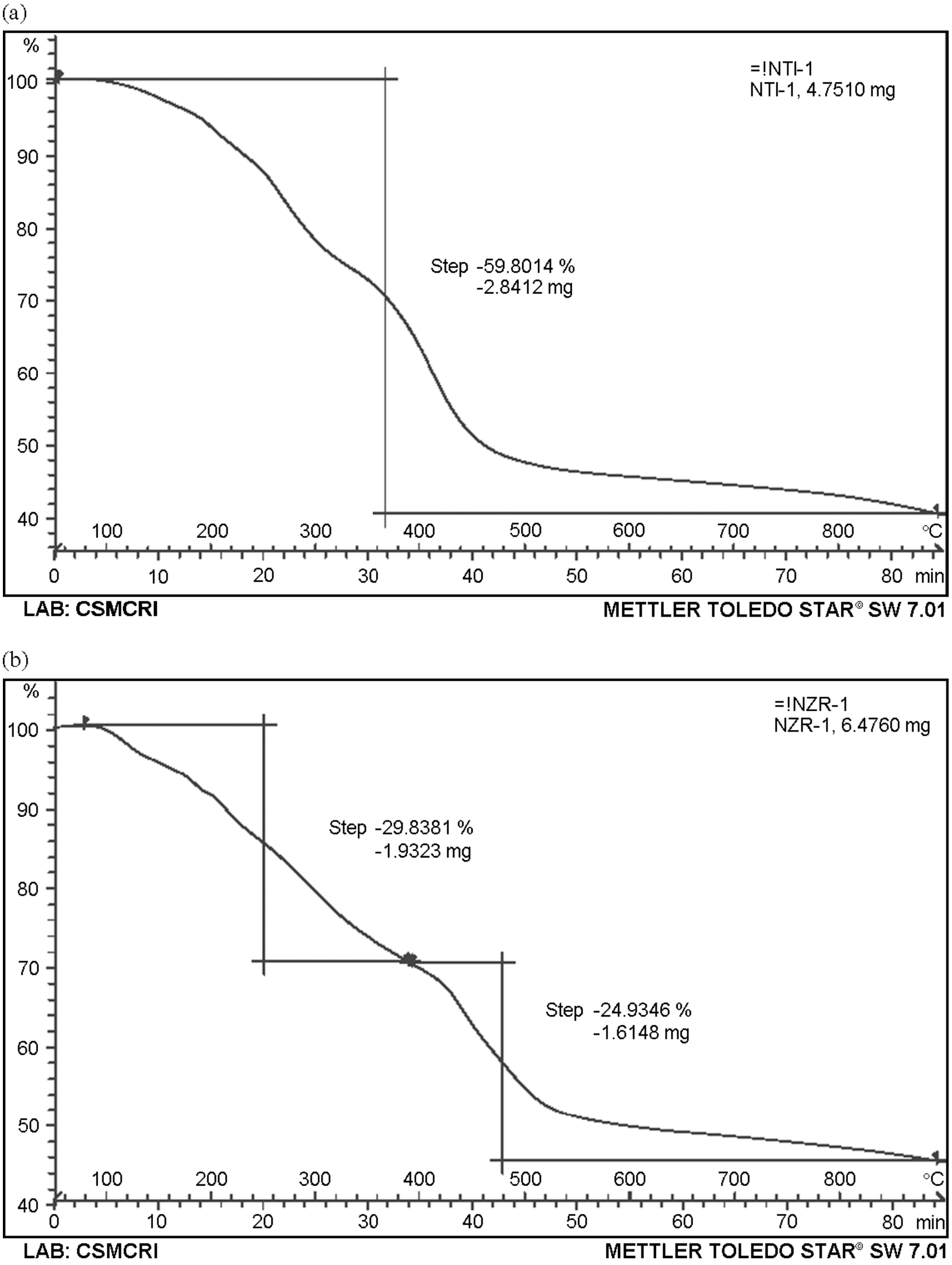

Figure 2. TGA curves (weight % vs temperature, °C) of (a) **1** and (b) **7**.

formation of large dense TiO_2 while those of sample **2**(600 °C) exhibit relatively less dense and smaller crystalline TiO_2 (by the contrast of BSE images). In the SEM image of sample **2,** the formation of fine grains is observed while for sample **1,** the formation of clearly demarcated grains is seen.

EXPERIMENTAL

All manipulations (expect hydrolysis) for synthesis and characterization of complexes were carried out under strictly anhydrous conditions. Solvents were dried by conventional methods and distilled prior to use. The Schiff's bases were prepared and purified using literature methods.[31] Metals were estimated as their dioxides and chloride was estimated by Volhard's method.[43] Microanalyses were performed on a Hereus Carlo Erba 1108 analyzer. The IR spectra were recorded on a Shimadzu FTIR 8400 spectrometer using KBr powder in the range 4000–400 cm^{-1}. The ^1H and $^{13}C\{^1H\}$ NMR spectra were collected in $CDCl_3$ solution using TMS as internal standard on a Jeol FX 300 FT NMR spectrometer at 300.4 and 75.45 IHz frequencies for ^1H and $^{13}C\{^1H\}$

DOI: 10.1002/aoc

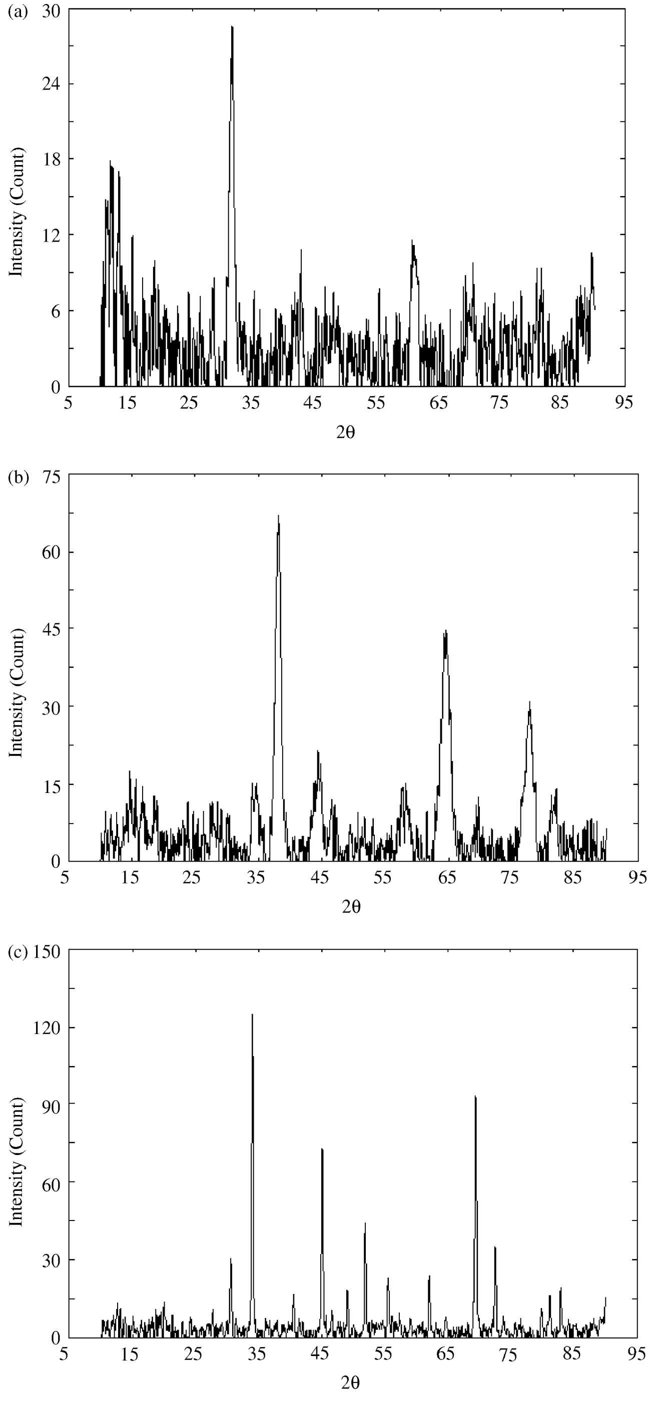

Figure 3. XRD of (a) pure TiO_2 obtained from **2** sintered at 600 °C, (b) pure ZrO_2 obtained from **7** sintered at 600 °C and (c) pure TiO_2 obtained from **1** sintered at 900 °C.

NMR, respectively. FAB mass spectra were obtained on a Jeol SX 102/DA-6000 mass spectrometer using *m*-nitrobenzyl alcohol matrix. Molecular weight measurements of titanocene complexes were carried out by determining depression in freezing point of benzene using Beckmann's Thermometer (Einstellthermometer n-Bek). XRD patterns were obtained on a Philips-1840 diffractometer using Fe source at λ 1.937 ´Å. The SEM images were obtained using a Philips XL30 scanning electron microscope. The samples were spread on a conducting carbon tape and images were recorded at magnifications of 1000× to 2000×, 20 kV, 10 mm working distance and spot size 4. Thermogravimetric analysis was performed on Mettler Toledo Star SW 701 with the heating rate 25–900/10 °C under N_2 atmosphere.

Preparation of $Cp_2Ti(Cl)\{OC(CH_3)=CHC(C_6H_5)=NPh\}$

Solid $NaOC(CH_3)=CHC(C_6H_5)=NPh$ (2.14 g, 8.25 mmol, prepared by the reaction of 0.19 g, 8.26 mmol of Na with 1.96 g, 8.25 mmol of Schiff's base in methanol) was added to a THF solution (~40 ml) of Cp_2TiCl_2 (2.06 g, 8.27 mmol). The reaction mixture was continuously stirred with refluxing for about 7 h. The precipitated NaCl was filtered off and excess solvent was removed under reduced pressure to give a reddish brown solid (3.72 g), which was re-crystallized from dichloromethane–*n*-hexane mixture.

Preparation of $Cp_2Zr(Cl)\{OC(CH_3)=CHC(C_6H_5)=NPh\}$

Using the above procedure, solid $NaOC(CH_3)=CHC(C_6H_5)=NPh$ (1.56 g, 6.02 mmol, prepared by the reaction of 0.14 g, 6.01 mmol of Na with 1.43 g, 6.02 mmol of ligand in methanol) was added to a THF solution (~40 ml) of Cp_2ZrCl_2 (1.76 g, 6.02 mmol). The contents were stirred and refluxed for 7 h. The resulting NaCl was filtered off and the filtrate was concentrated *in vacuo* to give a brown solid (2.86 g), which was re-crystallized from dichloromethane–*n*-hexane mixture.

All the other bis(cyclopentadienyl) complexes of titanium and zirconium were prepared by a similar route with different Schiff's bases. Their physical and analytical data are given in Table 1.

Hydrolysis of $Cp_2TiCl\{O(C_6H_4)CH=NPh\}$ (1), $Cp_2Ti\{O(C_6H_4)CH=NPh\}_2$ (2) and $Cp_2ZrCl\{O(C_6H_4)CH=NPh\}$ (7)

For the complete hydrolysis of $Cp_2Ti\{O(C_6H_4)CH=NPh\}_2$ (**2**), 1.22 g of compound was dissolved in ~10 ml of dry THF and ~15 ml of isopropanol. The color changed from reddish brown to dirty yellow. To this 2 ml of ammonia and water were added. Again, some more water and 1 ml ammonia were added and the mixture stirred for 5 days. The whole mixture was dried in an oven (at ~100 °C) overnight, then washed several times with acetone–hexane mixture. It was again dried in the oven and then washed with distilled water. This powder was sintered at 600 °C for 2 h, and characterized as pure TiO_2 (C, 0.29%; H, nil; N, nil). The compound $Cp_2ZrCl\{O(C_6H_4)CH=NPh\}$ (**7**) was hydrolyzed by the same method and sintered at 600 °C to give pure ZrO_2 (C, 0.13%; H, 1.33% and N, nil). The compound $Cp_2TiCl\{O(C_6H_4)CH=NPh\}$ (**1**) was also hydrolyzed using similar path with the only being difference that no ammonia was added in this case. Sintering of the TiO_2 powder at

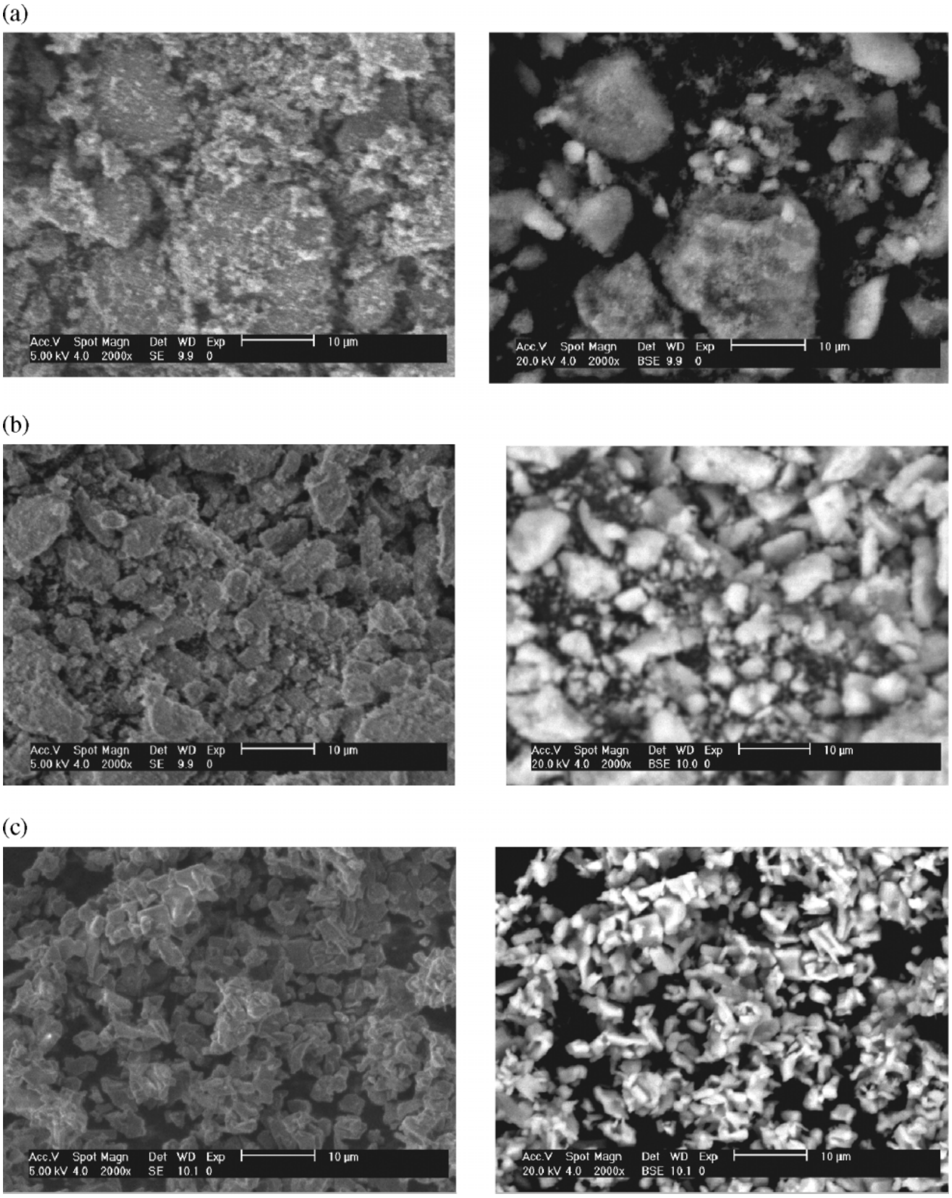

Figure 4. SEM images of (a) pure TiO_2 obtained from **2** sintered at 600 °C, (b) pure ZrO_2 obtained from **7** sintered at 600 °C and (c) pure TiO_2 obtained from **1** sintered at 900 °C.

600 °C afforded a white powder containing a black portion. Therefore, this was again sintered at higher temperatures and at 900 °C a completely white powder was obtained (C, 0.27%; H, 0.78% and N, nil).

CONCLUSION

Twelve new bis(cyclopentadienyl) Ti(IV) and Zr(IV) complexes with Schiff's base ligands were synthesized in THF in the absence of protonic nucleophilic medium such as methanol. All the reactions in THF are not only quantitative but also the products could be separated easily.[22] These complexes were characterized by FTIR, multinuclear NMR [^1H and $^{13}C\{^1H\}$] and FAB mass studies, indicating distorted tetrahedral coordination geometry around the central metal atom in solution. XRD and SEM images indicate the soft transformation of some of these complexes to pure nanosized titania or zirconia, suggesting their potential applications in material science.

Acknowledgment

We are grateful to UGC, CSIR and DST-New Delhi for financial support. V.S. thanks UGC for PDF. We thank the Department of Physics, University of Rajasthan, Jaipur, for XRD and CSMCRI, Bhavnagar for TGA.

DOI: 10.1002/aoc

REFERENCES

1. Bochmann M. *J. Chem. Soc., Dalton Trans.* 1996; 255.
2. Petasis NA, Lu SP, Bzowej EI, Fu DK, Staszewski JP, Zanze IA, Patane MA, Hu YH. *Pure Appl. Chem.* 1996; **68**: 667.
3. Arndt P, Spannenberg A, Baumann W, Becke S, Rosenthal U. *Eur. J. Inorg. Chem.* 2001; **11**: 2885.
4. Xu S, Deng X, Wang B, Zhou X, Yang L, Li Y, Hu Y, Zou F, Li Y. *Macro. Rapid Commun.* 2001; **22**: 708.
5. Weiβ T, Becke S, Sachse H, Rheinwald G, Lang H. *Inorg. Chem. Commun.* 2002; **5**: 159.
6. Qian Y, Huang J, Bala MD, Lian B. Zhang H, Zhang H. *Chem. Rev.* 2003; **103**: 2633.
7. Sanz M, Cuenca T, Galakhov M, Grassi A, Bott RKJ, Hughes DL, Lancaster SJ, Bochamann M. *Organometallics* 2004; **23**: 5324.
8. Miller SA, Bercaw JE. *Organometallics* 2004; **23**: 1777.
9. Kaminsky W. *J. Polym. Sci. Part A: Polym. Chem.* 2004; **42**: 3911.
10. Kuwabara J, Takeuchi D, Osakada K. *Organometallics* 2005; **24**: 2705.
11. Colacot TJ, Hosmane NS. *Z. Anorg. Allge. Chem.* 2005; **631**: 2659.
12. Merle PG, Chéron V, Hagen H, Lutz M, Spek AL, Deelman BJ, Koten GV. *Organometallics* 2005; **24**: 1620.
13. Möhring PC, Coville NJ. *Coord. Chem. Rev.* 2006; **250**: 18.
14. Köpf-Maier P, Hesse B, Väigtlande R, Köpf H. *J. Cancer Res. Clin. Oncol.* 1980; **97**: 31.
15. Tornieporth- Oetting IC, White PS. *Organometallics* 1995; **14**: 1632.
16. Guo M, Sun H, Bihari S, Parkinson JA, Gould RO, Parsons S, Sadler PJ. *Inorg. Chem.* 2000; **39**: 206.
17. Pandey OP, Sengupta SK, Mishra MK, Tripathi CM. *Bioinorg. Chem. Applic.* 2003; **1**: 35.
18. Meyer R, Brink S, Van Rensburg CEJ, Joone GK, Görls H, Lotz S. *J. Organomet. Chem.* 2005; **690**: 117.
19. Keeter G, Sweeney NJ, Strohfeldt K, Fiebig HH, Tacke M. *Anti-cancer Drugs* 2005; **16**: 1091.
20. Srivastava AK, Pandey OP, Sengupta SK. *Bioinorg. Chem. Applic.* 2005; **3**: 289.
21. Fichtner I, Pampillon C, Sweeney NJ, Strohfeldt K, Tacke M. *Anti-cancer Drugs* 2006; **17**: 333.
22. Wark TA, Stephan DW. *Organometallics* 1989; **8**: 2836.
23. Firth AV, Stephan DW. *Inorg. Chem.* 1998; **37**: 4726.
24. Sung RCW, Courtenay S, Mcgarvey BR, Stephan DW. *Inorg. Chem.* 2000; **39**: 2542.
25. Edward DA, Mahan MF, Paget TJ, Summerhill NW. *Trans. Met. Chem.* 2001; **26**: 116.
26. Matsuzaki K, Kawaguchi H, Voth P, Noda K, Itoh S, Takagi HD, Kashiwabara K, Tatsumi K. *Inorg. Chem.* 2003; **42**: 5320.
27. Chen X, Liu FC, Plečnik CE, Liu S, Du B, Meyers EA, Shore SG. *Organometallics* 2004; **23**: 2100.
28. Rosenthal U, Burlakov VV, Arndt P, Baumann W, Spannenberg A, Shur VB. *Eur. J. Inorg. Chem.* 2004; **24**: 4739.
29. Lee S, Seo KC, Yun SS, Kang SK. *J. Coord. Chem.* 2005; **58**: 695.
30. Aucott SM, Killian P, Milton HL, Robertson SD, Slawin AMZ, Woollins JD. *Inorg. Chem.* 2005; **44**: 2710.
31. Cozzi PG. *Chem. Soc. Rev.* 2004; **33**: 410.
32. Sharma N, Sharma RK, Bohra R, Drake JE, Hursthouse MB, Light ME. *J. Chem. Soc., Dalton Trans.* 2002; 1631.
33. Sharma N, Sharma RK, Bohra R. *J. Chem. Res.* 2003; 622.
34. Bohra R. *J. Indian Chem. Soc.* 2005; **82**: 197.
35. Jain AK, Gupta A, Bohra R, Lorenz IP, Mayer P. *Polyhedron* 2006; **25**: 654.
36. Agrawal S, Sharma V, Bohra R. *J. Chem. Res.* 2006; 426.
37. Sharma N, Sharma V, Bohra R, Raju VS, Lorenz IP, Krinninger C, Mayer P. *Inorg. Chim. Acta*. DOI: 10.1016/j.ica.2007.02.048.
38. Spijksma GI, Bouwmeester HJM, Blank DHA, Kessler VG. *Chem. Commun.* 2004; 1.
39. Casado MA, Torrente JJP, Ciriano MA, Edwards AJ, Lahoz FJ, Oro LA. *Organometallics* 1999; **18**: 5290.
40. Petrella AJ, Roberts NK, Craig DC, Raston CL, Lamb RN. *Chem. Commun.* 2003; 1014.
41. Roesky HW, Leichtweis I, Noltemeyer M. *Inorg. Chem.* 1993; **32**: 5102.
42. Warren BE. *X-Ray Diffraction*, Chap.13. Dover:, New York, 1990.
43. Vogel AI. *A Text Book of Quantitative Inorganic Analysis*, 5th edn. Longman: London, 1989.

DOI: 10.1002/aoc